Hindawi
Advances in Mathematical Physics
Volume 2020, Article ID 6185391, 8 pages
https://doi.org/10.1155/2020/6185391

Research Article

Weakly Coupled B-Type Kadomtsev-Petviashvili Equation: Lump and Rational Solutions

Na Xiong,[1] Wen-Tao Li,[2] and Biao Li[2]

[1] *College of Science and Technology, Ningbo University, Ningbo 315211, China*
[2] *School of Mathematics and Statistics, Ningbo University, Ningbo 315211, China*

Correspondence should be addressed to Biao Li; libiao@nbu.edu.cn

Received 12 June 2020; Accepted 27 July 2020; Published 30 September 2020

Academic Editor: Zine El Abiddine Fellah

Through the method of Z_N-KP hierarchy, we propose a new $(3+1)$-dimensional weakly coupled B-KP equation. Based on the bilinear form, we obtain the lump and rational solutions to the dimensionally reduced cases by constructing a symmetric positive semidefinite matrix. Then, we do numerical analysis on the rational solutions and fit the trajectory equation of the crest. Furthermore, we verify the accuracy of the trajectory equation by numerical analysis. This method of solving the lump and rational solutions can also be applied to other nonlinear evolution equations.

1. Introduction

During the recent years, in the field of nonlinear evolution equations, the exact solution is also widely concerned, such as the rational solutions, lump solutions, hybrid solutions, and rogue wave solutions [1–5]. And it has been applied to many fields: solid-state physics, fluid dynamics, plasma physics, and other nonlinear engineering problems. Furthermore, constructing exact solutions for nonlinear evolution equations is important in many scientific or engineering applications. Therefore, a series of systematic approaches, the Lie group method [6], Bäcklund transformation method, Darboux transformation method [7–10], Hirota bilinear method [11–13], inverse scattering transform method [14], and other methods [15], have been rapidly developed. It is meaningful and interesting to search for solutions to nonlinear evolution equations.

In this paper, the $(3+1)$-dimensional B-KP equation is expressed as

$$u_{xxxy} + \alpha\left(u_x u_y\right)_x + \left(u_x + u_y + u_z\right)_t - \left(u_{xx} + u_{zz}\right) = 0. \quad (1)$$

The B-KP equation describes the evolution of quasi-one-dimensional shallow water waves, when the effects of surface tension and viscosity are negligible and these are widely used in various physics fields such as the surface and internal oceanic waves, nonlinear optics, plasma physics, ferromagnetics, Bose-Einstein condensation, and string theory. Because of its importance, many properties have been studied. Wazwaz [16] established one and two soliton solutions of this equation by using the simplified Hereman-Nuseir form. Huang et al. [17] derived the bilinear Bäcklund transformations and soliton solutions to Equation (1); Bright-Dark lump wave solutions for a new form of the $(3+1)$-dimensional B-KP-Boussinesq equation have been explored in [18]. Lump, breather, and solitary wave solutions to the new reduced form of the generalized B-KP equation have been found in [19], and the dynamical analysis of lump solutions is exhibited in [20].

Based on bilinear derivatives, the B-KP equation can be transformed into the following bilinear equation:

$$\left(D_x^3 D_y + D_x D_t + D_y D_t + D_z D_t - D_x^2 - D_z^2\right) f \cdot f = 0, \quad (2)$$

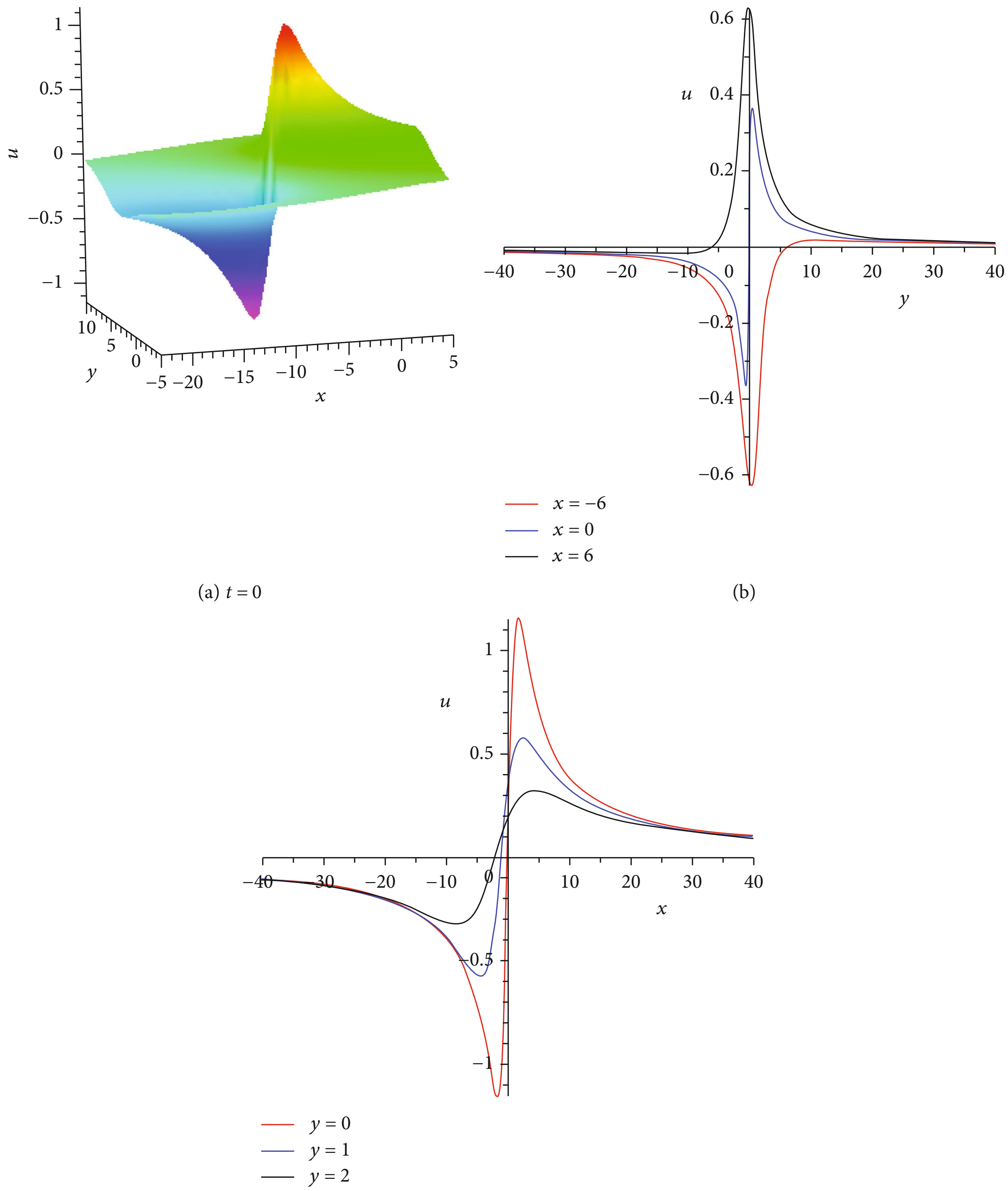

(a) $t = 0$

(b)

(c)

Figure 1: (Color online) The lump solution u to Equation (6) at $\alpha = 3$. (a) Contour plot. (b) x-curve. (c) y-curve.

under a dependent variable transformation

$$u(x, y, z, t) = \frac{6}{\alpha}(\ln f)_x. \tag{3}$$

The operator D is the Hirota bilinear differential operator, which is defined by

$$D_x^m D_t^n f \cdot g = \left(\frac{\partial}{\partial x} - \frac{\partial}{\partial x'}\right)^m \left(\frac{\partial}{\partial t} - \frac{\partial}{\partial t'}\right)^n f(x, y, z, t) \cdot g(x, y, z, t)|_{x'=x, t'=t}. \tag{4}$$

By taking the Z_N-KP hierarchy method [21], a new (3 + 1)-dimensional weakly coupled B-KP equation can be derived in the following form:

$$\begin{cases} u_{xxxy} + \alpha\left(u_x u_y\right)_x + \left(u_x + u_y + u_z\right)_t - \left(u_{xx} + u_{zz}\right) = 0, \\ v_{xxxy} + \alpha\left(v_x u_y\right)_x + \alpha\left(u_x v_y\right)_x + \left(v_x + v_y + v_z\right)_t - \left(v_{xx} + v_{zz}\right) = 0. \end{cases} \tag{5}$$

Equation (5) will be reduced to the following (2 + 1)-dimensional weakly coupled B-KP equation under $z = x$:

$$\begin{cases} u_{xxxy} + \alpha\left(u_x u_y\right)_x + \left(2u_x + u_y\right)_t = 0, \\ v_{xxxy} + \alpha\left(v_x u_y\right)_x + \alpha\left(u_x v_y\right)_x + \left(2v_x + v_y\right)_t = 0. \end{cases} \tag{6}$$

In this work, we mainly explore the lump and rational solutions to weakly coupled B-KP Equation (6). The rest of the paper is arranged as follows. In Section 2, the bilinear formalism of $(2+1)$-dimensional weakly coupled B-KP equation is derived. In Section 3, we obtain the lump and rational solutions to this equation by constructing symmetric positive semidefinite matrices, and some properties of the lump solutions are analyzed and discussed. Furthermore, we get the trajectory equation of the crest by using numerical analysis methods. Finally, our conclusion is presented in Section 4.

2. Bilinear Formalism

We start from a potential field f to construct bilinear transformation

$$\begin{cases} u = \dfrac{6}{\alpha}(\ln f)_x, \\ v = \dfrac{6}{\alpha}\left(\dfrac{g}{f}\right)_x. \end{cases} \tag{7}$$

By substituting u and v into Equation (6), the result is presented as

$$\begin{cases} 2f_{xxxy} - 2f_{xxx}f_y - 6f_{xxy}f_x + 6f_{xx}f_{xy} + 4f_{tx}f - 4f_x f_t + 2f_{ty} - 2f_y f_t - 4f_{xx}f + 4f_x^2 = 0, \\ f_{xxxy}g - f_{xxx}g_y - 3f_{xxy}g_x + 3f_{xx}g_{xy} + 3f_{xy}g_{xx} - 3f_x g_{xxy} - f_y g_{xxx} + f g_{xxxy} + 2f_{tx}g - 2f_x g_t - 2f_t g_x + 2f g_{tx} + f_{ty}g - f_y g_t - f_t g_y + f g_{ty} - 2f_{xx}g + 4f_x g_x - 2f g_{xx} = 0. \end{cases} \tag{8}$$

Equation (6) becomes the Hirota bilinear equation:

$$\begin{cases} \left(D_x^3 D_y + 2D_x D_t + D_y D_t - 2D_x^2\right) f \cdot f = 0, \\ \left(D_x^3 D_y + 2D_x D_t + D_y D_t - 2D_x^2\right) f \cdot g = 0, \end{cases} \tag{9}$$

where f and g are real functions with respect to variables x, y, and t and the operator D is the Hirota bilinear operate.

3. Lump Solutions and Rational Solutions

3.1. Lump Solutions. In order to obtain rational solutions to Equation (6), we set

$$\begin{cases} f = X^T A X + c_1, \\ g = X^T B X + c_2, \end{cases} \tag{10}$$

with

$$A = \begin{bmatrix} a_{11} & a_{12} & a_{13} \\ a_{12} & a_{22} & a_{23} \\ a_{13} & a_{23} & a_{33} \end{bmatrix}, \quad B = \begin{bmatrix} b_{11} & b_{12} & b_{13} \\ b_{12} & b_{22} & b_{23} \\ b_{13} & b_{23} & b_{33} \end{bmatrix}, \quad X = \begin{bmatrix} x \\ y \\ t \end{bmatrix}, \tag{11}$$

where a_{ij}, b_{ij}, and c_i are the real parameters that need to be determined; the matrices A and B are symmetric matrices.

After directly utilizing Maple symbolic calculation with f, a series of constraint equations for parameters are as follows:

$$\begin{aligned} a_{11} &= a_{11}, \\ a_{12} &= \frac{2a_{11}c_1(a_{11} - a_{13})}{3\,{a_{11}}^2 + a_{13}c_1}, \\ a_{13} &= a_{13}, \\ a_{22} &= \frac{4a_{11}(a_{11} - a_{13})\left(3{a_{11}}^2 + a_{11}c_1 - a_{13}c_1\right)}{a_{13}\left(3{a_{11}}^2 + a_{13}c_1\right)}, \\ a_{23} &= \frac{2(a_{11} - a_{13})\left(-3{a_{11}}^2 + a_{13}c_1\right)}{3{a_{11}}^2 + a_{13}c_1}, \\ a_{33} &= \frac{a_{13}\left(3{a_{11}}^2 + a_{13}c1\right)}{a_{11}(3a_{11} + c_1)}, \\ c_1 &= c_1. \end{aligned} \tag{12}$$

By combining Equations (10)–(12), the f is presented as follows:

$$\begin{aligned} f = {} & \frac{1}{a_{11}a_{13}(3a_{11} + c_1)\left(3a_{11}^2 + a_{13}c_1\right)}\left(36a_{11}^6 y^2 + a_{11}^5\left(\left(-36yt + 9x^2 - 36y^2\right)a_{13}\right.\right. \\ & \left. + 24y^2 c_1\right) + a_{11}^4\left(9t(t + 2x + 4y)a_{13}^2 - 12c_1 a_{13}\left(3y^2 + (t - x)y - \frac{x^2}{4} - \frac{3}{4}\right)\right. \\ & \left. + 4y^2 c_1^2\right) + 6\left(\left(2y^2 + (4t - 2x)y + x\left(t + \frac{x}{2}\right)\right)a_{13} + \frac{2c_1}{3}\left(xy - 2y^2 + \frac{3}{4}\right)a_{13}c_1 a_{11}^3\right. \\ & \left. + 6a_{13}^2 c_1 a_{11}^2\left(ta_{13}(t + x - 2y) + \frac{2c_1}{3}\left(y^2 + (t - x)y + \frac{x^2}{4} + \frac{3}{4}\right)\right)\right) \\ & \left. + 2a_{13}^2 c_1^2 a_{11}\left(a_{13}t(x - 2y) + \frac{c_1}{2}\right) + a_{13}^4 c_1^2 t^2\right). \end{aligned} \tag{13}$$

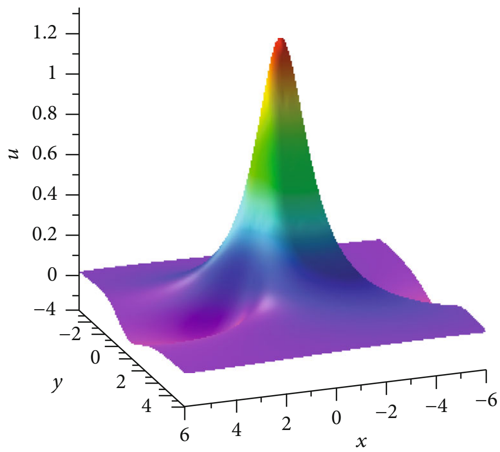

(a) $t = 0$

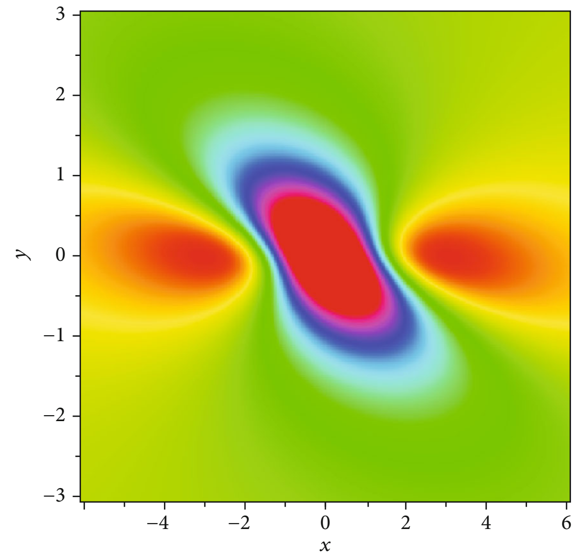

(b) $t = 0$

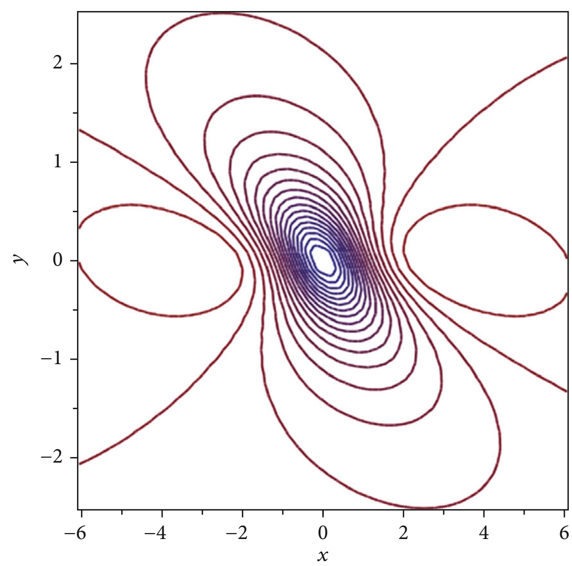

(c) $t = 0$

FIGURE 2: (Color online) The lump solutions v to Equation (6) at $\alpha = 3$. (b) Density plot of lump solution v. (c) Contour plot of lump solution v.

To obtain lump solutions u to Equation (6), the matrix A and parameter c_1 should satisfy the following conditions: (1) the matrix A must be a positive semidefinite matrix; (2) the real parameter c_1 must be greater than 0; (3) the elements of matrix A must also satisfy the following constraints $a_{11} > 0$ and $a_{11}a_{22} - a_{12}^2 > 0$. Among the above conditions, (1) and (2) are to ensure that f is always greater than 0. Condition (3) is to ensure that f has only one minimum at any time.

Under the above conditions, we found that we can take the following special parameter values:

$$\begin{aligned} a_{11} &= 3, \\ a_{13} &= 1, \\ c_1 &= 9. \end{aligned} \tag{14}$$

Substituting Equation (14) into f in Equation (7), we find

$$f = 2xt + 6xy - 4yt + 3x^2 + 30y^2 + 9 + \frac{2}{3}t^2. \tag{15}$$

Therefore, we obtain a lump solution of the $(2+1)$-dimensional B-KP Equation (6):

$$u = \frac{6(2t + 6y + 6x)}{\alpha\left(2xt + 6xy - 4yt + 3x^2 + 30y^2 + 9 + (2/3)t^2\right)}. \tag{16}$$

Table 1: The position of the crest of rational solution v_p.

t	x	y	h	$v_{p,x}$	$v_{p,y}$
70	-31.16593052	7.784650053	-72.77660922	-0.009991745	0.006720538
80	-35.60353148	8.894905304	-83.12405064	-0.006967661	0.004687028
90	-40.04265145	10.00535012	-93.47655836	-0.004985107	0.003357235
100	-44.48283519	11.11592780	-103.8325833	-0.003629698	0.002450331
110	-48.92379289	12.22660221	-114.1912831	-0.002679983	0.001809572
120	-53.36533119	13.33734922	-124.5519253	-0.001995900	0.001336341
130	-57.80731624	14.44815212	-134.9139212	-0.001486856	0.000991834
140	-62.24965236	15.55899896	-145.2777821	-0.001118218	0.000753025
150	-66.69226941	16.66988097	-155.6419954	-0.000837170	0.000580849
160	-71.13511472	17.78079155	-166.0064119	-0.000610380	0.000408621

Table 2: Test of the fitted equation.

t	x	y	h	$v_{p,x}$	$v_{p,y}$
-700	311.1166020	-77.77846821	725.9264744	-0.001726801	0.001024956
-600	266.6730730	-66.66747223	622.2330861	-0.002094850	0.001361426
-500	222.2299100	-55.55652233	518.5607668	-0.002483038	0.001668119
500	-222.2299068	55.55652118	-518.5267485	0.000035034	-0.000062859
600	-266.6730707	66.66747144	-622.2417001	-0.000208389	0.000347771
700	-311.1166004	77.77846763	-725.9318515	-0.000131428	-0.000185396

Figure 1 shows the contour plot, x-curve, and y-curve of the lump solution. And the lump solution u has a maxium point $(-(4/9)t+\sqrt{3},(1/9)t)$ and a minimum point $(-(4/9)t-\sqrt{3},(1/9)t)$. Besides, the lump solution reaches the maximum value of $(2\sqrt{3})/3$ and the minimum value of $-(2\sqrt{3})/3$.

We find a class of lump solutions to Equation (6). As mentioned above, since $u=(6/\alpha)(\ln f)_x$ is a lump solution to Equation (6), then we make $g=f_x$, so $v=(6/\alpha)(g/f)_x$ is also a lump solution to Equation (6). The correlative solutions are presented in the following form:

$$u=\frac{6(2t+6y+6x)}{\alpha\left(2xt+6xy-4yt+3x^2+30y^2+9+(2/3)t^2\right)},$$
$$v=\frac{-324\left(2xt+8yt+3x^2+6xy-24y^2-9\right)}{\alpha\left(2t^2+6xt-12yt+9x^2+18xy+90y^2+27\right)^2}. \quad (17)$$

As can be seen in Figure 2, when $\alpha=3$, the lump solution has a maximum point and two minimum points. The maximum value is obtained at $(-(4/9)t,(1/9)t)$, and the maximum value is 4/3; the minimum value is obtained at $(-(4/9)t+3,(1/9)t)$, $(-(4/9)t-3,(1/9)t)$, and the minimum value is $-1/6$.

3.2. Rational Solutions. In order to get the value of g and make the result clear, we substitute Equation (14) directly into Equation (8). And the related constraint equations are presented in the following form:

$$\begin{aligned}
b_{11}&=\frac{27\,b_{33}}{2}-9\,b_{13}+b_{12},\\
b_{12}&=b_{12},\\
b_{13}&=b_{13},\\
b_{22}&=28\,b_{12}-288\,b_{13}+351\,b_{33},\\
b_{23}&=28\,b_{13}-36\,b_{33}-2\,b_{12},\\
b_{33}&=b_{33},\\
c_2&=45\,b_{13}-54\,b_{33}.
\end{aligned} \quad (18)$$

Equation (18) contains three arbitrary parameters b_{12}, b_{13}, and b_{33}; we assign values to parameters as follows:

$$\begin{aligned}
b_{12}&=1,\\
b_{13}&=2,\\
b_{33}&=2.
\end{aligned} \quad (19)$$

The rational solution can be presented as

$$v_p=\frac{6}{\alpha}\left(\frac{g}{f}\right)_x, \quad (20)$$

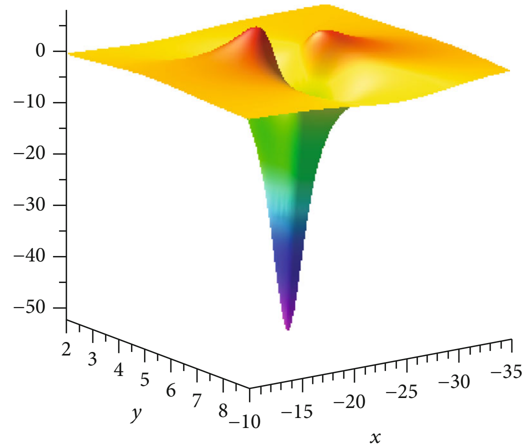

(a) $t = 50$

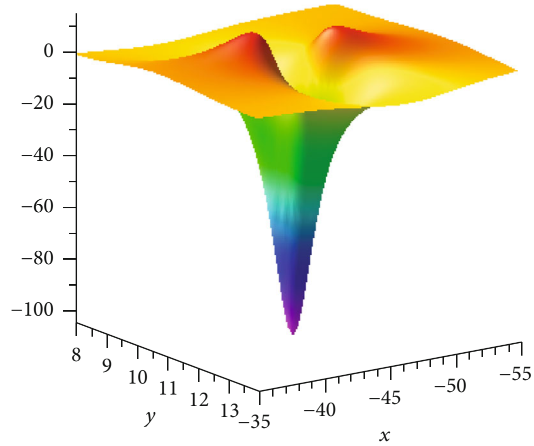

(b) $t = 100$

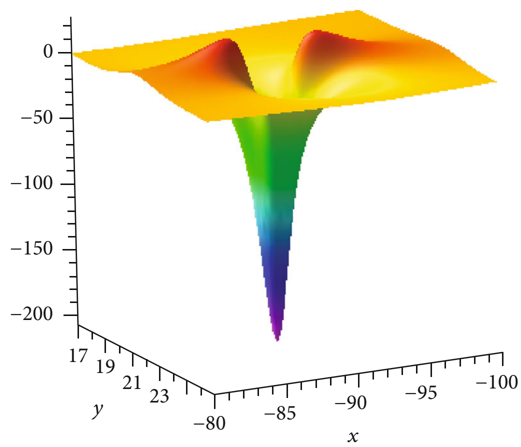

(c) $t = 200$

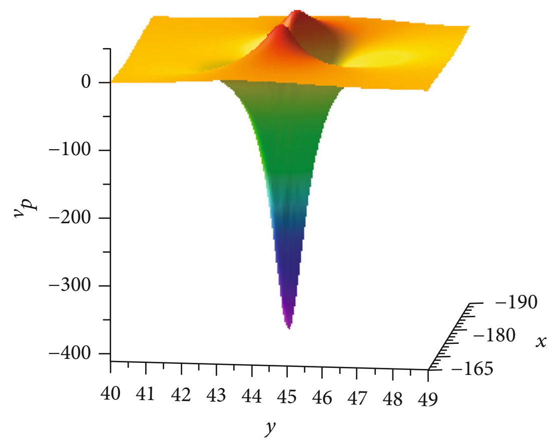

(d) $t = 400$

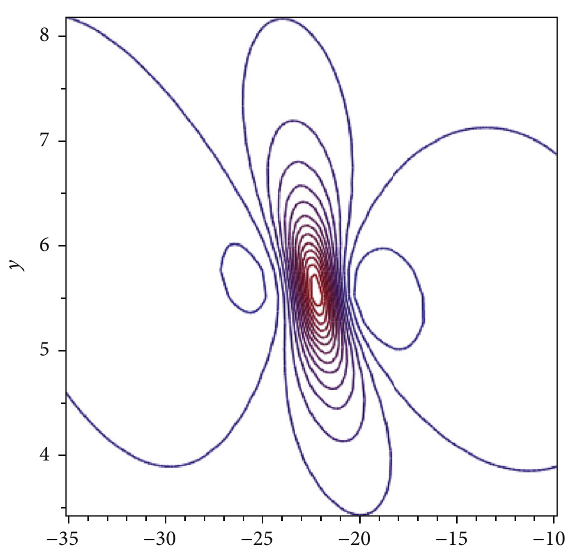

(e) $t = 50$

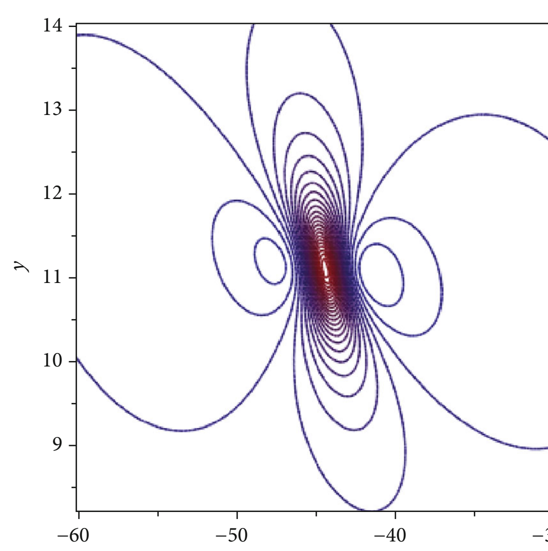

(f) $t = 100$

Figure 3: Continued.

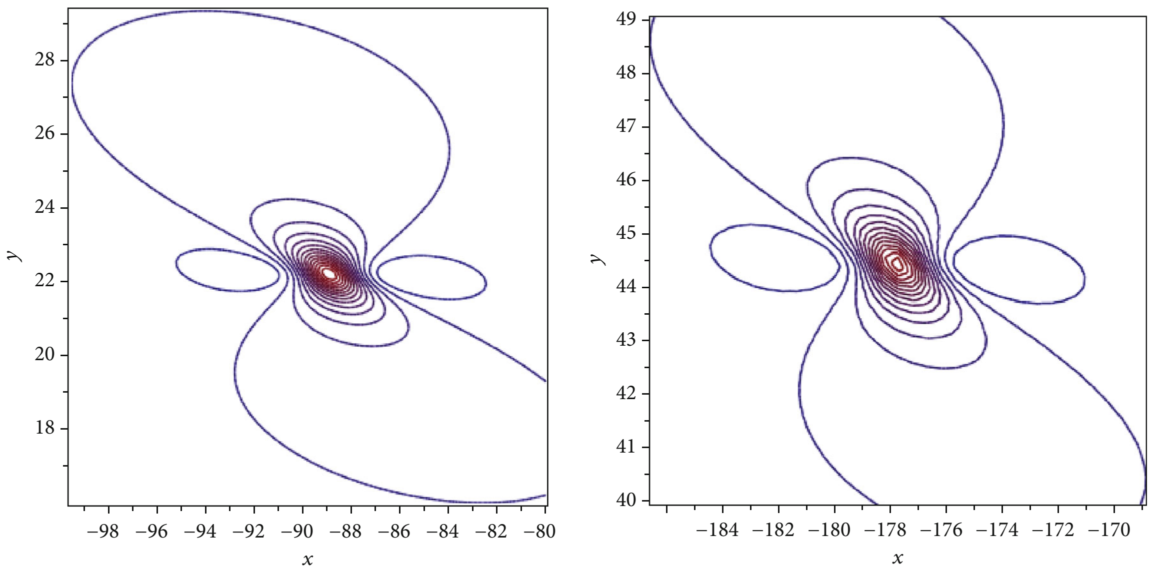

(g) $t = 200$ (h) $t = 400$

Figure 3: (Color online) The lump solutions v to Equation (6) at $\alpha = 3$.

with

$$\begin{aligned} f &= 9 + 6xy + 2xt - 4yt + 3x^2 + 30y^2 + \frac{2}{3}t^2, \\ g &= 2t^2 + 4xt - 36yt + 10x^2 + 2xy + 154y^2 - 18. \end{aligned} \tag{21}$$

Therefore, it can be seen from the above that v_p is the rational solution to Equation (6), and Equations (16) and (20) are a set of solutions to weakly coupled Equation (6).

After a detailed analysis, we find that rational solution v_p has some fascinating properties. This property is that v_p is an odd function, which means $v_p(-x,-y,-t) = -v_p(x,y,t)$. Therefore, when we know the trajectory of the crest at $t < 0$ at a certain period of time, we can know the corresponding trajectory of the crest at $t > 0$. We find that the solutions of $v_{p,x} = 0$ and $v_{p,y} = 0$ have extremely complex algebraic structures, so we do not know what curve of the crest is over time. Therefore, we investigate the motion trajectory of the rational solution by taking the numerical analysis method.

When $\alpha = 3$, the position of the crest at different times can be seen in Table 1. Here, h is the height of the crest and the $v_{p,x}$ and $v_{p,y}$ are used to measure the error of numerical calculation. When $v_{p,x}$ and $v_{p,y}$ are closer to 0, the position of the crest will be more accurate.

From the above description, we construct a nonlinear fit to the data in Table 1. During a certain period of time $t > 0$, the motion trajectory of this crest can be fitted to the following equation:

$$\begin{cases} x = \dfrac{-3.84308585121464619}{t + 0.104467282340778067} - \dfrac{4}{9}t, \\ y = \dfrac{0.483098011069225342}{t + 0.296660717750461933} + \dfrac{1}{9}t. \end{cases} \tag{22}$$

We find from Equation (22) that as the time increases gradually, the trajectory of the crest will fit more linearly. And, an interesting phenomenon that can be seen from Figure 2 is that the strange wave of v_p is very similar to the lump wave at every moment, and its amplitude and time are proportional. Since v_p is an odd function, we obtain the trajectory equation of v_p at $t < 0$ by combining Equation (23). So the result is presented in the following form:

$$\begin{cases} x = \dfrac{-3.84308585121464619}{t - 0.104467282340778067} - \dfrac{4}{9}t, \\ y = \dfrac{0.483098011069225342}{t - 0.296660717750461933} + \dfrac{1}{9}t. \end{cases} \tag{23}$$

Thus, Equations (22) and (23) can accurately express the trajectory of v_p at every moment. Next, we do some numerical tests on the equations in Equations (22) and (23). The results are presented in Table 2.

As can be seen from Table 2, when $t \in (-700,700)$, $v_{p,x}$ and $v_{p,y}$ are very close to 0, so it can be explained that Equations (22) and (23) can accurately represent the position of the crest.

4. Conclusion

In this paper, by using the Z_m-KP hierarchy, a new $(3+1)$-dimensional weakly coupled B-KP equation has been constructed. And its dimensionally reduced form has been investigated. We obtain the lump solutions to Equation (6) by taking the Hirota bilinear method and constructing the symmetric positive semidefinite matrix technique. The lump solutions are displayed in three-dimensional graphics (see Figures 1 and 2). We also found an interesting set of rational solutions u, v_p to Equation (6) by using the same method. And the height of v_p will also increase proportionally over time. Time-varying rational solutions are presented in graphics (see Figure 3). By taking a numerical analysis of the rational solution v_p, the motion trajectory of v_p is approximately linear motion over time (see Table 1). And we also test the equations of the moving trajectory by using numerical analysis methods. The position and fitting results of the trajectory equation are presented (see Table 2). In this paper, the method of finding the lump and rational solutions to weakly coupled B-KP equations by constructing a symmetric positive semidefinite matrix can also be applied to other nonlinear evolution equations. We hope that our results can provide valuable help in the field of nonlinear science.

Data Availability

No data were used to support this study.

Conflicts of Interest

The authors declare that they have no conflicts of interest.

Acknowledgments

This work is supported by the National Natural Science Foundation of China under Grant Nos. 11805106, 11775121, and 11435005 and the K.C.Wong Magna Fund in Ningbo University.

References

[1] H. Zhou, C. Li, and Y.-L. Lin, "Rational solutions of a weakly coupled nonlocal nonlinear Schrödinger equation," *Advances in Mathematical Physics*, vol. 2018, Article ID 9216286, 12 pages, 2018.

[2] M. Chen, X. Li, Y. Wang, and B. Li, "A pair of resonance stripe solitons and lump solutions to a reduced (3+1)-dimensional nonlinear evolution equation," *Communications in Theoretical Physics*, vol. 67, pp. 595–600, 2017.

[3] Z. Wang and X. Liu, "Bifurcations and exact traveling wave solutions for the KdV-like equation," *Nonlinear Dynamics*, vol. 95, no. 1, pp. 465–477, 2019.

[4] Y. K. Liu and B. Li, "Nonlocal symmetry and exact solutions of the (2+1)-dimensional Gardner equation," *Chinese Journal of Physics*, vol. 54, no. 5, pp. 718–723, 2016.

[5] X. E. Zhang and Y. Chen, "Rogue wave and a pair of resonance stripe solitons to a reduced (3+1)-dimensional Jimbo-Miwa equation," *Communications in Nonlinear Science and Numerical Simulation*, vol. 52, pp. 24–31, 2017.

[6] A. H. Abdel Kader, M. S. Abdel Latif, and Q. Zhou, "Exact optical solitons in metamaterials with anti-cubic law of nonlinearity by Lie group method," *Optical and Quantum Electronics*, vol. 51, no. 1, p. 30, 2019.

[7] Y. Zhang, J. W. Yang, K. W. Chow, and C. F. Wu, "Solitons, breathers and rogue waves for the coupled Fokas-Lenells system via Darboux transformation," *Nonlinear Analysis: Real World Applications*, vol. 33, pp. 237–252, 2017.

[8] X. G. Geng, J. Wei, and B. Xue, "A coupled nonlinear Schrödinger-type equation and its Darboux transformation," *Modern Physics Letters B*, vol. 32, no. 17, article 1850192, 2018.

[9] Z. X. Zhou, "Darboux transformations and global solutions for a nonlocal derivative nonlinear Schrödinger equation," *Communications in Nonlinear Science and Numerical Simulation*, vol. 62, pp. 480–488, 2018.

[10] X. W. Yan, S. F. Tian, M. J. Dong, and T. T. Zhang, "Rogue waves and their dynamics on bright-dark soliton background of the coupled higher order nonlinear Schrödinger equation," *Journal of the Physical Society of Japan*, vol. 88, no. 7, article 074004, 2019.

[11] W. X. Ma and Y. Zhou, "Lump solutions to nonlinear partial differential equations via Hirota bilinear forms," *Journal of Differential Equations*, vol. 264, no. 4, pp. 2633–2659, 2018.

[12] C. Y. Qin, S. F. Tian, X. B. Wang, T. T. Zhang, and J. Li, "Rogue waves, bright-dark solitons and traveling wave solutions of the (3+1)-dimensional generalized Kadomtsev-Petviashvili equation," *Computers & Mathematcs with Applications*, vol. 75, no. 12, pp. 4221–4231, 2018.

[13] W. Q. Peng, S. F. Tian, T. T. Zhang, and Y. Fang, "Rational and semi-rational solutions of a nonlocal (2 + 1)-dimensional nonlinear Schrödinger equation," *Mathematical Methods in the Applied Sciences*, vol. 42, no. 18, pp. 6865–6877, 2019.

[14] W. X. Ma, "The inverse scattering transform and soliton solutions of a combined modified Kortewegde Vries equation," *Journal of Mathematical Analysis and Applications*, vol. 471, no. 1, pp. 476–811, 2019.

[15] E. Topp and M. Yangari, "Weakly coupled systems of parabolic Hamilton-Jacobi equations with Caputo time derivative," *Nonlinear Differential Equations and Applications NoDEA*, vol. 25, no. 5, article 41, 2018.

[16] A. M. Wazwaz, "Two forms of (3+1)-dimensional B-type Kadomtsev-Petviashvili equation: multiple soliton solutions," *Physica Scripta*, vol. 86, no. 3, article 035007, 2012.

[17] Z. R. Huang, B. Tian, H. L. Zhen, J. Yan, Y. P. Wang, and Y. Sun, "Bäcklund transformations and soliton solutions for a (3 + 1) -dimensional B-type Kadomtsev-Petviashvili equation in fluid dynamics," *Nonlinear Dynamics*, vol. 80, no. 1-2, pp. 1–7, 2015.

[18] L. Kaur and A. M. Wazwaz, "Bright-dark lump wave solutions for a new form of the (3 + 1)-dimensional BKP-Boussinesq equation," *Romanian Reports in Physics*, vol. 71, pp. 1–11, 2018.

[19] L. Kaur and A. M. Wazwaz, "Lump, breather and solitary wave solutions to new reduced form of the generalized BKP equation," *International Journal of Numerical Methods for Heat & Fluid Flow*, vol. 29, no. 2, pp. 569–579, 2018.

[20] L. Kaur and A. M. Wazwaz, "Dynamical analysis of lump solutions for (3 + 1) dimensional generalized KP-Boussinesq equation and its dimensionally reduced equations," *Physica Scripta*, vol. 93, no. 7, article 075203, 2018.

[21] C. Li and J. He, "The extended Z N -Toda hierarchy," *Theoretical and Mathematical Physics*, vol. 185, no. 2, pp. 1614–1635, 2015.